63-4-

AFCRL-63-623

THE UNIVERSITY OF CHICAGO

DEPARTMENT OF THE GEOPHYSICAL SCIENCES

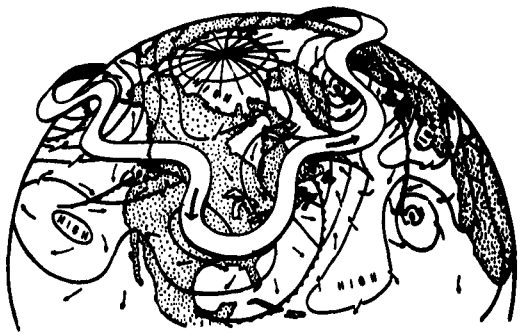

ON THE INFLUENCE OF RELEASED LATENT HEAT ON CYCLONE DEVELOPMENT

by

Maurice B. Danard

Weather Forecasting Research Center

Contract No. AF 19(604)-7230

Project No. 8641

Task No. 86410

Scientific Report No. 10

June 1963

Prepared for

AIR FORCE CAMBRIDGE RESEARCH LABORATORIES
OFFICE OF AEROSPACE RESEARCH
UNITED STATES AIR FORCE
BEDFORD, MASSACHUSETTS

AFCRL-63-623

THE UNIVERSITY OF CHICAGO

DEPARTMENT OF THE GEOPHYSICAL SCIENCES

ON THE INFLUENCE OF RELEASED LATENT HEAT ON CYCLONE DEVELOPMENT

by

Maurice B. Danard

Weather Forecasting Research Center

Contract No. AF 19(604)-7230

Project No. 8641

Task No. 86410

Scientific Report No. 10

June 1963

Prepared for

AIR FORCE CAMBRIDGE RESEARCH LABORATORIES
OFFICE OF AEROSPACE RESEARCH
UNITED STATES AIR FORCE
BEDFORD, MASSACHUSETTS

Requests for additional copies by Agencies of the Department of Defense, their contractors, and other Government agencies should be directed to the:

DEFENSE DOCUMENTATION CENTER (DDC)
ARLINGTON HALL STATION
ARLINGTON 12, VIRGINIA

Department of Defense contractors must be established for DDC services or have their 'need-to-know' certified by the cognizant military agency of their project or contract.

All other persons and organizations should apply to the:

U. S. DEPARTMENT OF COMMERCE
OFFICE OF TECHNICAL SERVICES
WASHINGTON 25, D.C.

TABLE OF CONTENTS

ABSTRACT

The influences of release of latent heat of vaporization on vertical motion, production of kinetic energy, and development of low-level vorticity have been investigated. The vertical motion was obtained by solving the customary (diagnostic) omega-equation, making allowance for horizontal variations of the static stability. The results were compared with vertical velocities computed by kinematical techniques, and it was found that it was necessary to include the effect of released latent heat in order to obtain satisfactory agreement between the two sets of data. Experimental computations showed that the effects of spatial variations of the static stability were important outside regions of condensation.

Numerical solutions, with and without inclusion of released latent heat, were used to obtain ageostrophic wind components and their effect upon the production of kinetic energy and vorticity. The following results emerged: (a) the influence of released latent heat was of the same order of magnitude as the effect of dry-adiabatic circulations; (b) to the amplification of the vertical motions that resulted from released latent heat corresponded intensification of the low-level convergence and high-level divergence; (c) the ageostrophic winds associated with these fields of convergence and divergence had components toward lower pressure, thus giving positive contributions to the production of kinetic energy both at low and at high levels; (d) the computed rate of production of low-level vorticity exceeded the observed rate, and evidence suggests that frictional effects may be important.

ACKNOWLEDGEMENTS

The author wishes to express his gratitude to Professor Sverre Petterssen for encouragement, advice and assistance in the preparation of this paper. Thanks are due also to Professors George W. Platzman and Tetsuya Fujita for many helpful suggestions; to Mr. Kaare Pedersen for advice during the early phase of the work; and to Mr. J. R. Fulks, Meteorologist-in-Charge, U. S. Weather Bureau District Center, Chicago, who made available the synoptic charts used in the case study.

LIST OF SYMBOLS

A	horizontal area
C	drag coefficient
C_p	specific heat of dry air at constant pressure
f	Coriolis parameter
f_o	areal mean value of f
g	acceleration of gravity
H	heat given to a unit mass per unit time
K	kinetic energy per unit mass of the horizontal motion
K_g	kinetic energy per unit mass of the geostrophic motion
K_g	total kinetic energy of the geostrophic motion of a system
L	lateral boundary of the horizontal area A
L_v	latent heat of vaporization of water
p	pressure
p_o	a standard pressure (=1000 mb)
q	vertical component of the relative vorticity $(= (\partial v/\partial x)_p - (\partial u/\partial y)_p)$
q_g	geostrophic relative vorticity $(\cong (g/f)\nabla^2 Z)$
r	mixing ratio
R	specific gas constant of dry air
T	temperature
T_d	dew-point temperature
u, v	components of the horizontal wind vector in the x- and y-directions, respectively
u_g, v_g	components of the geostrophic wind in the x- and y-directions, respectively

V	magnitude of the horizontal wind vector
V_g	magnitude of the geostrophic wind
V_o	wind speed at anemometer level
x, y	right-handed horizontal orthogonal coordinates
Z	height of an isobaric surface
α	specific volume of dry air
θ	potential temperature
ρ_o	air density at anemometer level
σ	a measure of the stability with respect to dry-adiabatic changes $\left(= -(\alpha/\theta)(\partial\theta/\partial p) \right)$
σ_o	areal mean value of σ
φ	velocity potential of the ageostrophic wind
Φ	geopotential of an isobaric surface
ω	vertical velocity expressed in terms of pressure $(= dp/dt)$
$\mathbb{F}$	frictional force per unit mass
$\mathbb{R}$	vertical unit vector
$\mathbb{V}$	horizontal wind vector
$\mathbb{V}_g$	geostrophic wind
$\mathbb{V}'$	irrotational component of the ageostrophic wind
∇	horizontal differential operator on an isobaric surface
∇^2	horizontal Laplacian operator on an isobaric surface

1. INTRODUCTION

During the Nineteenth Century many investigators (e. g. Reye 1872, and Ferrel 1889) maintained that the release of latent heat of vaporization contributed substantially to the development of cyclones, and some support for this thought was provided later when it became evident that the rate of release of latent heat far exceeded the production of kinetic energy. On the other hand, Margules (1903) calculated that, in a closed system, the increase in kinetic energy, resulting from the redistribution of juxtaposed warm and cold air masses, was negligibly affected by the occurrence of condensation in the warm air, provided the latter were potentially stable. It should be mentioned, however, that Margules considered only initial and final states and made no inference as to the rate of increase in kinetic energy. Furthermore, the assumption of closed boundaries would limit the application of his results to natural systems. It is, perhaps, due to Margules' influence that, in later years, little attention was paid to the importance of release of latent heat as source of energy in cyclone development. Only recently, mainly as a result of advances in numerical forecasting, has interest again become centered on the role of latent heat in the development of motion systems.

The purpose of this paper is to explore the manner in which release of latent heat affected the development of a selected cyclone. More specifically, we shall be concerned with the effects on the fields on vertical motion and divergence and the rates of production of kinetic energy and low-level vorticity.

2. SOME EARLIER INVESTIGATIONS

An early idea which has recurred frequently in the literature is that the release of latent heat of vaporization tends to decrease the density of the air column in which condensation occurs and thereby lower the pressure at the base of the column. Reye (1865) considered an atmospheric column with cross section of $1\ m^2$ in which 1 kg of water vapor at $10^{\circ}C$ was condensed, thereby producing 1 mm of precipitation. From the released latent heat he computed the horizontal expansion and found a pressure reduction of about 0.8 mb. This provided him with a relation between precipitation and surface pressure from which he concluded that the heat released by condensation was the chief cause of cyclone development. In a similar manner, Refsdal (1930) considered a saturated atmosphere with unstable stratification above the 800 mb level. By letting a parcel of air rise from 800 to 500 mb Refsdal found that a saturated-adiabatic lapse rate would become established in the ascending column and that, under such temperature conditions as normally prevail in middle latitudes, about 10 mm of precipitation would have been released. Refsdal assumed that the rising air would be about $5^{\circ}C$ warmer than its environment between 750 and 500 mb, and his calculations showed that if the height of the 500 mb surface remained constant the sea level pressure would be reduced by about 4.6 mb. Like Reye, Refsdal considered that he had obtained a valid relationship between the intensity of precipitation and the rate of fall of the sea-level pressure.

On the other hand, Hann (1874) studied records from Batavia and found that heavy rains (20 mm or more per hour) were accompanied by rising pressure, and from this he concluded that the release of latent heat could not account for the development of low-pressure systems. It may be noted, however, that the data examined by Hann likely reflected the effects

of downdrafts from convective clouds.

Fundamental progress in the understanding of the energy sources of cyclones was achieved by Margules (1903), whose influence is clearly evident in the later works of the Norwegian school of meteorologists. Margules considered first a double chamber (as shown on the left in Fig. 2. 2. 1) in which two masses of dry air in stable or neutral equilibrium, having the temperatures T_A and T_B (with $T_A < T_B$), were separated by a vertical wall. It was assumed that the pressure remained constant along the top surface and that the discontinuity in pressure at the partition increased from zero at the top to a maximum value at the bottom of the chamber. If the effects of friction are neglected and the boundaries assumed to be rigid, it is readily shown that

$$K + P + I - Q = \text{constant} \tag{2.2.1}$$

where K, P, and I denote the kinetic, potential, and internal energy, respectively, and Q is the heat added to the system.

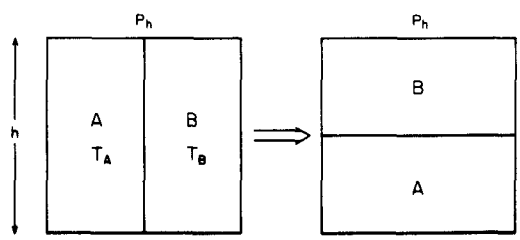

Fig. 2.2.1. Margules' two-chamber model.

When the partition between the chambers is removed the air masses will become redistributed as shown in the diagram on the right. If subscript a identifies an adiabatic process, the difference between the initial and the final states is found to be

$$\Delta K_a = -\Delta (P + I)_a \tag{2.2.2}$$

Furthermore, if the two chambers are of equal size, the following approximate relationship can be shown to hold

$$\Delta K_a = \frac{M}{2} g h \frac{T_B - T_A}{T_A} \tag{2.2.3}$$

where M is the total mass.

Margules next considered the effect when the mass B was replaced by saturated air having a saturated-adiabatic lapse rate. When the partition is now removed, condensation will take place in the mass B, and Eq. (2.2.1) gives

$$\Delta K_h = -\Delta (P + I)_h + Q \tag{2.2.4}$$

Here, subscript h signifies that the release of latent heat is involved.

Margules found that

$$-\left[\Delta (P + I)_a - \Delta (P+I)_h\right] = Q \tag{2.2.5}$$

showing that when condensation occurs, the decrease in potential and internal energy is less than it would have been had the process been dry-adiabatic, the difference being equal to the amount of released latent heat. Equation (2.2.5) may be interpreted to state that the release of latent heat of vaporization merely diminishes the rate of cooling of the ascending mass and does not contribute to the increase of kinetic energy. Thus

$$\Delta K_h = \Delta K_a \tag{2.2.6}$$

a result which might seem to defeat the main purpose of the present paper. It should be noted, however, that Margules did not consider the influence of the surroundings on the system, nor did he draw any conclusions about the rate at which the conversion of energy takes place; it is possible, and indeed probable, that the amplifying effect that release of latent heat has on the vertical motion may accelerate the conversion process. We shall return to the discussion of this in later sections.

In a second paper, Margules (1906) considered the case when the mass B is potentially unstable, and found a significant contribution from the released latent heat. In the following Sections 3 and 4, discussion will be restricted to cases where the air is potentially stable, and it will be shown that even in such cases release of latent heat may lead to significant increases in the kinetic energy of mid-latitude cyclones.

In connection with numerical predictions the vertical velocity is usually obtained by solving the so-called ω -equation derived by Fjörtoft (1955); a form of this equation will be reproduced in Section 3.1. In the early applications of Fjörtoft's equation it was customary to ignore the effects of released latent heat. It soon became evident, however, that the neglect of latent heat in the ω -equation resulted in a substantial underestimate of the

vertical motions within the regions where condensation occurred. The first attempt at accounting for the effect of condensation was made by Smagorinsky (1956) who found that the calculated velocities could be augmented by an order of magnitude, partly by accounting for the horizontal variation in the static stability but primarily by including the effect of release of latent heat. Other authors have also demonstrated the importance of released heat of vaporization in dynamical processes. For example, Manabe (1956) studied a case of heavy large-scale precipitation in which a considerable increase of potential vorticity occurred in the lower troposphere. He found that the increase in potential vorticity predicted from heat released by condensation was of the right order of magnitude to explain the observed changes. Furthermore, Aubert (1957) found that the released heat of vaporization greatly increased the upward motion, and he found that this release also tended to lower the heights of the isobaric surfaces in the lower troposphere and to raise them in the upper atmosphere. These changes resulted in deepening of low-level cyclones and acceleration of their rates of movement. Smebye (1958) conducted a number of experiments in quantitative precipitation forecasting; he included the effect of heat released by condensation and, except in the vicinity of convective systems, found good agreement between predicted and observed amounts of precipitation. Further refinements were introduced by Pedersen (1962) who, like Smebye, demonstrated the importance of the inclusion of released latent heat.

In a recent study of the effects of heat sources on the behavior of winter cyclones on the North Atlantic Ocean, Petterssen and collaborators (1962) computed the rate of change of the thickness from 1000 to 500 mb during typical stages of development of extra-tropical cyclones, and found that the inclusion of released latent heat as well as the eddy flux of sensible heat were important. In typical cases, the maximum flux of sensible heat occurred in the rear of the cyclone center and amounted to about 1 cal cm^{-2} min^{-1}. Since a rate of precipitation of 1 mm hr^{-1} would liberate an equivalent amount of heat, it is evident that, when the temperature is high, the release of latent heat may be of paramount importance.

3. THEORY AND PROCEDURE

The purpose of this section is to present the basic theory and an outline of the procedure to be employed. Further details of the methods used will be discussed in Section 4.

3.1 Vertical Velocity

With the symbols defined elsewhere, the quasi-geostrophic vorticity equation and the corresponding thermodynamic energy equation may be written:

$$\frac{\partial q_g}{\partial t} + V_g \cdot \nabla (q_g + f) = f_o \frac{\partial \omega}{\partial p} \tag{3.1.1}$$

and

$$\zeta \frac{\partial}{\partial t} \frac{\partial z}{\partial p} + \zeta V_g \cdot \nabla \frac{\partial z}{\partial p} + \sigma \omega = - \frac{R H}{C_p p} \tag{3.1.2}$$

It may be noted that Eq. (3.1.1) satisfies the consistency requirements of Hollmann (1956), Wiin-Nielsen (1959), and Lorenz (1960), provided variations in q_g and V_g arising from changes in f are neglected. However, Eq. (3.1.2) does not satisfy these criteria, unless for each isobaric surface σ is taken to be a constant, and H is defined such that

$$\int H \zeta A = 0$$

The above integral is to be taken over the area in question. Nevertheless,

as will be shown in Section 4, the use of an inconsistent form of Eq. (3.1.2) represents the instantaneous physical relations better than does the consistent form, although the use of the former in numerical forecasting may cause spurious energy changes after a large number of time steps.

Combining Eqs. (3.3.1) and (3.1.2), we obtain

$$\nabla^2\sigma\omega + ff_0\frac{\partial^2\omega}{\partial p^2} = -g\nabla^2\mathbf{V}_g\cdot\nabla\frac{\partial z}{\partial p} + f\frac{\partial}{\partial p}\mathbf{V}_g\cdot\nabla(q_g+f) - \frac{R}{c_p p}\nabla^2 H \tag{3.1.3}$$

The above equation represents a simplification of the ω -equation derived by Fjörtoft (1955).

Since Eq. (3.1.3) is linear in ω , we may write

$$\omega = \omega_a + \omega_h$$

where ω_a may be interpreted as the vertical velocity due to dry-adiabatic processes, and ω_h as the additional velocity caused by non-adiabatic heating. Equation (3.1.3) may then be replaced by the following two equations:

$$\nabla^2\sigma\omega_a + ff_0\frac{\partial^2\omega_a}{\partial p^2} = -g\nabla^2\mathbf{V}_g\cdot\nabla\frac{\partial z}{\partial p} + f\frac{\partial}{\partial p}\mathbf{V}_g\cdot\nabla(q_g+f) \tag{3.1.4}$$

and

$$\nabla^2\sigma\omega_h + ff_0\frac{\partial^2\omega_h}{\partial p^2} = -\frac{R}{c_p p}\nabla^2 H \tag{3.1.5}$$

In Sections 4.3 and 4.4, the above two equations will be solved by relaxation techniques, using a vertical mesh size of 200 mb and keeping the dependent variable zero at $p = 0$ and at $p = 1000$ mb. The two solutions will then be added to give ω. For comparison, the vertical velocity will also be determined kinematically, taking orographic influences into account. Ageostrophic, frictional and orographic effects neglected in the numerical solution and errors inherent in the kinematic technique will be the main factors preventing an exact agreement between the two results.

The main contribution to H will be assumed to be from heat released by condensation, and other heat sources and sinks will be neglected. Furthermore, it will be assumed that condensation occurs as liquid water which immediately falls out as precipitation. Apart from the question of the phase of the condensed water substance, this last assumption is at variance with the conclusions of Cunningham (1952). He found that in cases of steady rain, appreciable amounts of water are collected when precipitation elements produced by clouds aloft fall through low-level stratus and scud. These low clouds owe their existence not to large-scale vertical motion but rather to evaporation from falling rain and from the earth's surface. However, if the former moisture source is more important than the latter, Cunningham's results should not seriously affect the validity of our assumption. This is because the loss of water by evaporation of falling rain (which has been neglected) will be compensated by a gain when the raindrops fall through the low clouds.

To determine the spatial distribution of H, use will be made of the vertical velocity as computed kinematically and the observed precipitation rates, both averaged over areas centered at grid points (see Fig. 4.3.1). It will be assumed that condensation occurs only in the region between 900 and 300 mb. The atmosphere will be divided into layers 200 mb deep centered at 800, 600 and 400 mb, and the moisture data from radio soundings will be used to determine which of these layers could readily produce precipitation. For

convenience, a possible precipitation-producing layer will be defined as one which contains sub-layers where $T - T_d \leq 5^\circ C$. This figure has been chosen somewhat arbitrarily to make allowance for the fact that 100 per cent relative humidity is rarely reported by radiosondes even in cases of continuous rain. Let the subscripts i and m denote conditions at the i^{th} grid point and m^{th} level (m = 1, 2, 3 correspond to 800, 600 and 400 mb respectively). At each grid point, we have

$$-\epsilon_i \sum_{m=1}^{3} C_{im}(T,p)\,\omega_{im}\,\delta_m = P_i \tag{3.1.6}$$

where P_i is the total precipitation and $C_{im}(T, p)$ is the precipitation produced by a 200 mb deep saturated layer ascending at the rate of 10^{-3} mb sec^{-1} (obtained by modifying values given by Fulks, 1935). The quantity δ_m is defined alternatively as follows:

δ_m = 1 if the m^{th} layer has sufficient moisture to produce precipitation and $\omega_{im} < 0$; otherwise

δ_m = 0

Since ω_{im} is known from kinematic computations, Eq. (3.1.6) can be solved for ϵ_i , which is the fraction of the column that is producing precipitation (if $\delta_1 = \delta_2 = \delta_3 = 1$, $\epsilon_i = 1$ indicates saturation from 900 to 300 mb). Having found ϵ_i , H_{im} is determined from

$$H_{im} = -\frac{g}{200\ mb}\,\epsilon_i\, C_{im}(T,p)\,\omega_{im}\,L_v\,\delta_m \tag{3.1.7}$$

The quantity 200 mb/g is the mass of a column of air of unit area and 200 mb depth so H_{im} is the rate of heating per unit mass. Hence, Eqs. (3.1.3) or (3.1.5) can now be solved.

An alternative way to solve Eq. (3.1.3) is the following. If ω_{im} in Eq. (3.1.7) is interpreted as the solution of Eq. (3.1.3) rather than the kinematically determined vertical velocity, Eq. (3.1.3) may be written

$$\nabla^2(\sigma-\sigma_s)\omega + ff_0\frac{\partial^2\omega}{\partial p^2} = -g\nabla^2 V_g\cdot\nabla\frac{\partial z}{\partial p} + f\frac{\partial}{\partial p}V_g\cdot\nabla(q_g+f) \tag{3.1.8}$$

where

$$\sigma_s = \frac{R}{C_p p}\frac{g}{200\ mb}\epsilon_i C_{im}(T,p)L_v\delta_m \tag{3.1.9}$$

There are two difficulties in the way of obtaining solutions to Eq. (3.1.8) rather than Eqs. (3.1.3) or (3.1.5). In the first place, the unknown ϵ_i cannot be determined until Eq. (3.1.8) has been solved for ω. If we make an initial guess of ϵ_i, Eq. (3.1.6) will not be satisfied unless our initial guess were correct. Secondly, Eq. (3.1.8) will not have a bounded solution if $\sigma - \sigma_s \leq 0$. Furthermore, since numerical methods will be used, large errors may result if $\sigma - \sigma_s$, though positive, is close to zero. Of course, if $\sigma - \sigma_s < 0$, the atmosphere is unstable and the pattern of vertical motion takes the form of small-scale convective cells. In this case, the solutions of Eqs. (3.1.3), (3.1.4) or (3.1.5) may have little meaning. However, instability should manifest itself in the precipitation pattern, and if this pattern is fairly uniform, it may be concluded that the solutions of Eqs. (3.1.3), (3.1.4) or (3.1.5) then represent real atmospheric processes.

3.2 Changes in Kinetic Energy

Following Phillips (1956), we multiply Eq. (3.1.1) by $-\zeta_g Z/f$, neglect small terms arising from the variations of f, and obtain the quasi-geostrophic energy equation

$$\frac{\partial k_g}{\partial t} = -\nabla \cdot k_g \mathbf{V}_g - \frac{\partial}{\partial p}\Phi\omega - \omega\alpha \tag{3.2.1}$$

where $k_g = (u_g^2 + v_g^2)/2$ is the kinetic energy per unit mass of the geostrophic motion.

On the other hand, multiplying scalarly by $\mathbf{V}$ the equation of frictionless motion

$$\frac{d\mathbf{V}}{dt} = -\nabla\Phi - f\mathbf{k}\times\mathbf{V} \tag{3.2.2}$$

one obtains

$$\frac{\partial k}{\partial t} = -\nabla\cdot(k+\Phi)\mathbf{V} - \frac{\partial}{\partial p}(k+\Phi)\omega - \omega\alpha \tag{3.2.3}$$

where $k = (u^2+v^2)/2$ is the kinetic energy of the horizontal motion per unit mass.

The wind field will be assumed to be composed of a geostrophic component $\mathbf{V}_g$ and a small irrotational perturbation $\mathbf{V}'$ given by

$$\mathbf{V}' = -\nabla\Phi \tag{3.2.4}$$

where the velocity potential φ satisfies the condition

$$\nabla^2\varphi = \frac{\partial \omega}{\partial p} \tag{3.2.5}$$

It has been postulated here that the geostrophic wind contains all the vorticity, and Petterssen (1953) has shown that, on occasions, this is not justified. However, this assumption has been made in order to obtain a convenient separation of the motion into geostrophic and ageostrophic components. Moreover, the effect discussed by Petterssen is important only in cases where the deformation is strong and the vorticity weak.

Substituting $\mathbb{V} = \mathbb{V}_g + \mathbb{V}'$ into Eq. (3.2.2) and proceeding as before, we obtain the approximate energy equation

$$\frac{\partial k_g}{\partial t} = -\nabla\cdot k_g\mathbb{V}_g - \nabla\cdot\Phi\mathbb{V}' - \frac{\partial}{\partial p}(k_g + \Phi)\omega - \omega\alpha \tag{3.2.6}$$

which, by virtue of its similarity to Eq. (3.2.3), will represent the physical conditions better than does Eq. (3.2.1).

An alternate expression to Eq. (3.2.6) is

$$\frac{\partial k_g}{\partial t} = -\nabla\cdot k_g\mathbb{V}_g - \frac{\partial}{\partial p}k_g\omega - \mathbb{V}'\cdot\nabla\Phi \tag{3.2.7}$$

If Eq. (3.2.7) is integrated over a region bounded at the top and bottom by the pressure levels p_t and p_b, respectively, we obtain

$$\frac{\partial K_g}{\partial t} = -\int\oint V_{gn}\, k_g\, \delta L\, \frac{\delta p}{g} + \int\left[(k_g\omega)_{p_t} - (k_g\omega)_{p_b}\right]\frac{\delta A}{g} - \int\int \mathbf{V}'\cdot\nabla\Phi\, \delta A\, \frac{\delta p}{g} \tag{3.2.8}$$

where

$$K_g = \int\int k_g\, \delta A\, \frac{\delta p}{g}$$

is the total kinetic energy of the geostrophic motion within the region, and V_{gn} is the component of $\mathbf{V}_g$ along the exterior normal to the lateral boundary L.

Equation (3.2.8) thus gives the rate of change of the kinetic energy of the geostrophic motion within the region. The first two integrals on the right represent the net horizontal and vertical import of kinetic energy into the region. The last term is the rate of working by the pressure forces within the region.

Equation (3.2.8) may now be divided into three parts: one which is due to purely geostrophic motion; one which is due to ageostrophic effects arising from dry-adiabatic processes; and one which is caused by released latent heat. From the solutions of Eqs. (3.1.4) and (3.1.5) and Eqs. (3.2.4) and (3.2.5), we find $\mathbf{V}'_a$ and $\mathbf{V}'_h$, the ageostrophic wind components caused by dry-adiabatic processes and released heat of vaporization, respectively. The three components of Eq. (3.2.8), denoted by the subscripts g, a and h, respectively, may then be written:

$$\left[\frac{\partial K_g}{\partial t}\right]_g = -\int\oint V_{gn}\, k_g\, \delta L\, \frac{\delta p}{g} \tag{3.2.9}$$

$$\left[\frac{\partial K_s}{\partial t}\right]_a = \int\left[(k_s\omega_a)_{p_t} - (k_s\omega_a)_{p_b}\right]\frac{\delta A}{g} - \int\int V_a'\cdot\nabla\Phi\,\delta A\,\frac{\delta p}{g} \tag{3.2.10}$$

$$\left[\frac{\partial K_s}{\partial t}\right]_h = \int\left[(k_s\omega_h)_{p_t} - (k_s\omega_h)_{p_b}\right]\frac{\delta A}{g} - \int\int V_h'\cdot\nabla\Phi\,\delta A\,\frac{\delta p}{g} \tag{3.2.11}$$

An equivalent though less simple approach would be to integrate Eq. (3.2.6). Analogous to Eq. (3.2.8) we would then obtain

$$\begin{aligned}\frac{\partial K_s}{\partial t} = &-\int\oint V_{sn}\,k_s\,\delta L\,\frac{\delta p}{g} + \int\left[(k_s\omega)_{p_t} - (k_s\omega)_{p_b}\right]\frac{\delta A}{g} \\ &-\int\oint V_n'\,\Phi\,\delta L\,\frac{\delta p}{g} + \int\left[(\Phi\omega)_{p_t} - (\Phi\omega)_{p_b}\right]\frac{\delta A}{g} \\ &-\int\int\omega\alpha\,\delta A\,\frac{\delta p}{g}\end{aligned} \tag{3.2.12}$$

where V_n' is the normal component of V'.

The third and fourth integrals on the right side of Eq. (3.2.12) represent the rate of working by the pressure forces on the boundaries of the region. It is readily shown (e.g., White and Saltzman, 1956) that the last term is the rate of conversion of potential and internal energy into kinetic energy.

Expressions equivalent to Eqs. (3.2.10) and (3.2.11) are

$$\left[\frac{\partial K_g}{\partial t}\right]_a = \int\left[(k_g\omega_a)_{p_t} - (k_g\omega_a)_{p_b}\right]\frac{\delta A}{g} - \int\oint V'_{na}\,\Phi\,\delta L\,\frac{\delta p}{g}$$

$$+\int\left[(\Phi\omega_a)_{p_t} - (\Phi\omega_a)_{p_b}\right]\frac{\delta A}{g} - \int\int\omega_a\alpha\,\delta A\,\frac{\delta p}{g} \tag{3.2.13}$$

$$\left[\frac{\partial K_g}{\partial t}\right]_h = \int\left[(k_g\omega_h)_{p_t} - (k_g\omega_h)_{p_b}\right]\frac{\delta A}{g} - \int\oint V'_{nh}\,\Phi\,\delta L\,\frac{\delta p}{g}$$

$$+\int\left[(\Phi\omega_h)_{p_t} - (\Phi\omega_h)_{p_b}\right]\frac{\delta A}{g} - \int\int\omega_h\alpha\,\delta A\,\frac{\delta p}{g} \tag{3.2.14}$$

The chief difficulty in the way of using Eqs. (3.2.13) and (3.2.14) rather than Eqs. (3.2.10) and (3.2.11), is encountered in calculating the integrals

$$-\int\oint V'_{na}\,\Phi\,\delta L\,\frac{\delta p}{g}$$

and

$$-\int\oint V'_{nh}\,\Phi\,\delta L\,\frac{\delta p}{g}$$

Since these terms depend only upon the values of V'_a and V'_h on the borders of the region, it is likely that the boundary error in the numerical solution of these induced velocities will adversely affect the results. Consequently, in Section 4.5 the terms in the kinetic energy equation will be evaluated using Eqs. (3.2.9) to (3.2.11) and only the last terms in Eqs. (3.2.13) and (3.2.14) will be calculated.

3.3 Low-Level Vorticity Production

If the complete vorticity equation

$$\frac{d}{dt}(q+f) = -(q+f)\nabla\cdot\mathbf{V} - \mathbf{k}\cdot\nabla\omega\times\frac{\partial\mathbf{V}}{\partial p} + \mathbf{k}\cdot\nabla\times\mathbf{F} \tag{3.3.1}$$

is applied to a vorticity maximum (i.e., $\nabla(q+f) = 0$) at a level where ω is small, one obtains

$$\frac{\delta}{\delta t}(q+f) = -(q+f)\nabla\cdot\mathbf{V} + \mathbf{k}\cdot\nabla\times\mathbf{F} \tag{3.3.2}$$

Here $\delta/\delta t$ is the local change in a coordinate system moving with the vorticity maximum.

Let us now consider a level within the friction layer but sufficiently far from the ground for the following conditions to hold:

$$q \cong q_g \tag{3.3.3}$$

and

$$-\nabla\cdot\mathbf{V} \cong \frac{\partial\omega_a}{\partial p} + \frac{\partial\omega_h}{\partial p} \tag{3.3.4}$$

Here, ω_a and ω_h are solutions to Eqs. (3.1.4) and (3.1.5).

Using Eqs. (3.3.3) and (3.3.4), Eq. (3.3.2) may be divided into two components:

(3.3.5) $$\left[\frac{\delta}{\delta t}(q_g+f)\right]_a = (q_g+f)\frac{\partial \omega_a}{\partial p} + \mathbb{k}\cdot\nabla\times\mathbb{F}$$

(3.3.6) $$\left[\frac{\delta}{\delta t}(q_g+f)\right]_h = (q_g+f)\frac{\partial \omega_h}{\partial p}$$

where the subscripts a and h refer to dry- and saturated- adiabatic processes, respectively. The terms in the above equations will be computed in Section 4.6.

A method of estimating the order of magnitude of the frictional term in Eq. (3.3.5) will now be described. The frictional force will be assumed to be expressible in the form

(3.3.7) $$\mathbb{F} = -b\mathbb{V}$$

where $\nabla b = 0$. We then have

$$\mathbb{k}\cdot\nabla\times\mathbb{F} = -bq$$

and, using Eq. (3.3.3),

(3.3.8) $$\mathbb{k}\cdot\nabla\times\mathbb{F} = -bq_g$$

To determine $\mathbf{F}$, consider a column of unit area extending from the ground to a height of 1 km. The magnitude of the stress on the bottom surface of the column is assumed to be given by

$$F_o = \rho_o C V_o^2 \tag{3.3.9}$$

and the stress on the top surface will be neglected. The average force per unit mass is then approximately

$$F = (10^{-5} cm^{-1}) C V_o^2 \tag{3.3.10}$$

which will be assumed to be also the magnitude of $\mathbf{F}$ at the level in question. Comparing Eqs. (3.3.7) and (3.3.10), it will be seen that

$$b = \frac{(10^{-5} cm^{-1}) C V_o^2}{V} \tag{3.3.11}$$

Combining Eqs. (3.3.8) and (3.3.11), we then obtain

$$\mathbf{k} \cdot \nabla \times \mathbf{F} = - \frac{(10^{-5} cm^{-1}) C V_o^2}{V} q_s \tag{3.3.12}$$

The fact that a linear function of the velocity has been used in Eq. (3.3.7) while a quadratic one is used in Eq. (3.3.10) is not as inconsistent as would appear on first sight. We have only required that $\nabla b = 0$ in Eq. (3.3.7) and if $\nabla V = 0$ also, we can set

$$b = b' V$$

Eq. (3.3.7) then becomes

$$\mathbb{F} = -b' \nabla \mathbb{V}$$

It is interesting to note that it is possible to determine the effect of released latent heat on Petterssen's development equation (Petterssen, 1955). Integrating Eq. (3.1.2) from p , the level of non-divergence, to p_o we have

$$g \frac{\partial}{\partial t} Z_{p_o} = g \frac{\partial}{\partial t} Z_p - g \int_p^{p_o} V_g \cdot \nabla \frac{\partial Z}{\partial p} \delta p - \int_p^{p_o} \sigma \omega \, \delta p$$

(3.3.13)

$$- \int_p^{p_o} \frac{R}{C_p p} H \, \delta p$$

where Z_{p_o} and Z_p are the heights of the pressure surfaces p_o and p respectively. Applying the operator $(1/f)\nabla^2$ to Eq. (3.3.13) and setting

$$\frac{\partial}{\partial t} \frac{g}{f} \nabla^2 Z_p = - \left[V_g \cdot \nabla (q_g + f) \right]_p$$

we obtain

$$\frac{\partial}{\partial t} \frac{g}{f} \nabla^2 Z_{p_o} = - \left[V_g \cdot \nabla (q_g + f) \right]_p - \frac{g}{f} \int_p^{p_o} \nabla^2 V_g \cdot \nabla \frac{\partial Z}{\partial p} \delta p$$

(3.3.14)

$$- \frac{1}{f} \int_p^{p_o} \nabla^2 \sigma \omega \, \delta p - \frac{1}{f} \int_p^{p_o} \frac{R}{C_p p} \nabla^2 H \, \delta p$$

which is Petterssen's development equation with the geostrophic approximation used to represent the vorticity and the advective wind.

It is customary to treat H in Eq. (3.3.14) as heat introduced from external sources and, in cases of saturated ascent, deal with released latent heat by modifying $\nabla^2 \sigma\omega$ in Eq. (3.3.14) to

$$\nabla^2\left[\sigma - \frac{R}{C_p p}\,\frac{L_v}{1+r_s}\left(\frac{dr}{dp}\right)_s\right]\omega$$

Here, the subscript s denotes the saturated state. The term $(R/C_p p)(L_v/(1+r_s))(dr/dp)_s$ is equivalent to the right side of Eq. (3.1.9). However, external heat sources will be neglected here and H will be interpreted as released heat of vaporization.

Writing $\omega = \omega_a + \omega_h$ and making use of Eq. (3.1.5), Eq. (3.3.14) may be written

$$\frac{\partial}{\partial t}\frac{g}{f}\nabla^2 z_{p_o} = -\left[V_g\cdot\nabla(q_g+f)\right]_p - \frac{g}{f}\int_p^{p_o}\nabla^2 V_g\cdot\nabla\frac{\partial z}{\partial p}\delta p$$

(3.3.15)

$$+\frac{1}{f}\int_p^{p_o}\nabla^2\sigma\omega_a\delta p + f_o\left(\frac{\partial\omega_h}{\partial p}\right)_{p_o}$$

The last term in Eq. (3.3.15) represents the effect of released latent heat and, had $(q_g+f)(\partial\omega/\partial p)$ been used on the right side of Eq. (3.1.1), this term would be $\left[(q_g+f)(\partial\omega_h/\partial p)\right]_{p_o}$.

Substituting Eq. (3.1.4) in the third term on the right side of Eq. (3.3.15), one obtains

$$\frac{\partial}{\partial t}\ \frac{g}{f}\nabla^2 z_{p_o} = -\left[\mathbf{V}_g\cdot\nabla(q_g+f)\right]_{p_o} + f_o\left(\frac{\partial\omega_a}{\partial p}\right)_{p_o} + f_o\left(\frac{\partial\omega_h}{\partial p}\right)_{p_o} \tag{3.3.16}$$

If the vorticity advection at 1000 mb is small, it is evident that the effects of dry- and saturated-adiabatic processes are proportional to $(\partial\omega_a/\partial p)_{p_o}$ and $(\partial\omega_h/\partial p)_{p_o}$, respectively. This result is similar to that expressed by Eqs. (3.3.5) and (3.3.6).

Substituting Eq. (3.1.4) in the third term on the right side of Eq. (3.3.15), one obtains

$$\frac{\partial}{\partial t}\frac{g}{f}\nabla^2 Z_{p_o} = -\left[V_g\cdot\nabla(q_g+f)\right]_{p_o} + f_o\left(\frac{\partial\omega_a}{\partial p}\right)_{p_o} + f_o\left(\frac{\partial\omega_h}{\partial p}\right)_{p_o} \tag{3.3.16}$$

If the vorticity advection at 1000 mb is small, it is evident that the effects of dry- and saturated-adiabatic processes are proportional to $(\partial\omega_a/\partial p)_{p_o}$ and $(\partial\omega_h/\partial p)_{p_o}$, respectively. This result is similar to that expressed by Eqs. (3.3.5) and (3.3.6).

4. A CASE STUDY

4.1 General Synopsis

The case selected for study was a cyclone which developed rapidly over the central United States on January 21-22, 1959 (Fig. 4.1.1). The system was associated with an intense baroclinic zone and was accompanied by widespread heavy precipitation.

During the period 0000-1200 GMT of the 21st the frontal low moved from western Texas to southeastern Missouri, becoming more organized but filling slightly. Shortly after 1200 GMT the system began to deepen at the rate of approximately 1 mb hr^{-1}. By 0000 GMT of the 22nd it had reached southern Ontario and had then developed into a major cyclone. From the 500 mb map in the lower right of Fig. 4.1.1, it will be seen that, in accordance with Petterssen's development hypothesis (Petterssen, 1955), sudden development began when the area of appreciable vorticity advection in mid-troposphere spread over the low-level frontal zone.

An investigation of the dynamic and thermodynamic processes occurring in the atmosphere at the onset of sudden cyclogeneis should provide a better understanding of the complex phenomenon of cyclone development. It was therefore decided to perform the computations proposed in Section 3 using the data for 1200 GMT of the 21st.

Precipitation rates at 1200 GMT (Fig. 4.1.2) were obtained from the observed four-hour amounts ending at 1400 GMT which were then averaged over areas centered at grid points (see Fig. 4.3.1) and converted to hourly rates. The time and area averaging procedure resulted in the smooth pattern shown in Fig. 4.1.2. Note the elongation of the precipitation pattern along the

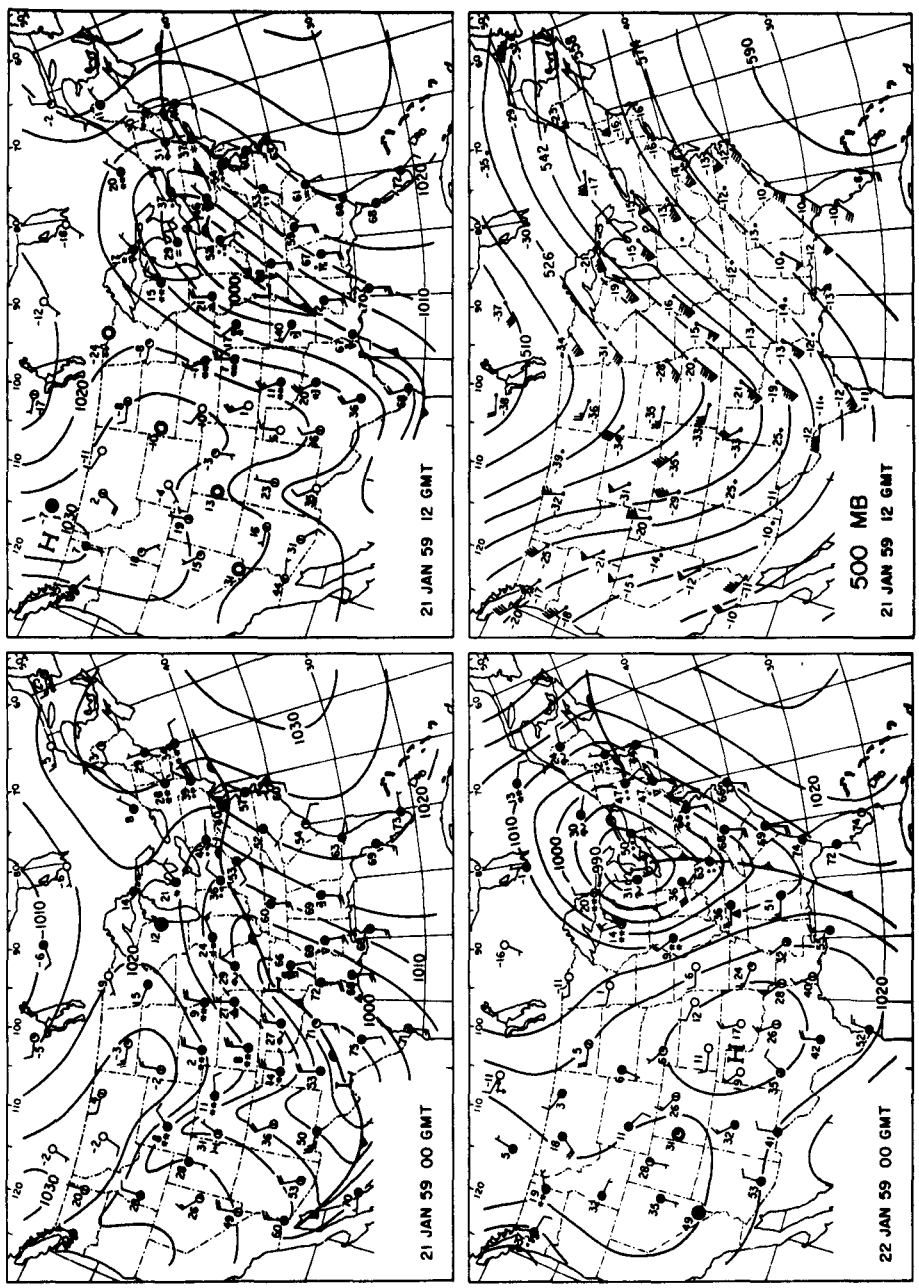

Fig. 4.1.1. Sequence of sea-level charts showing the development of a major cyclone. Lower right: 500 mb map at the onset of sudden cyclogenesis.

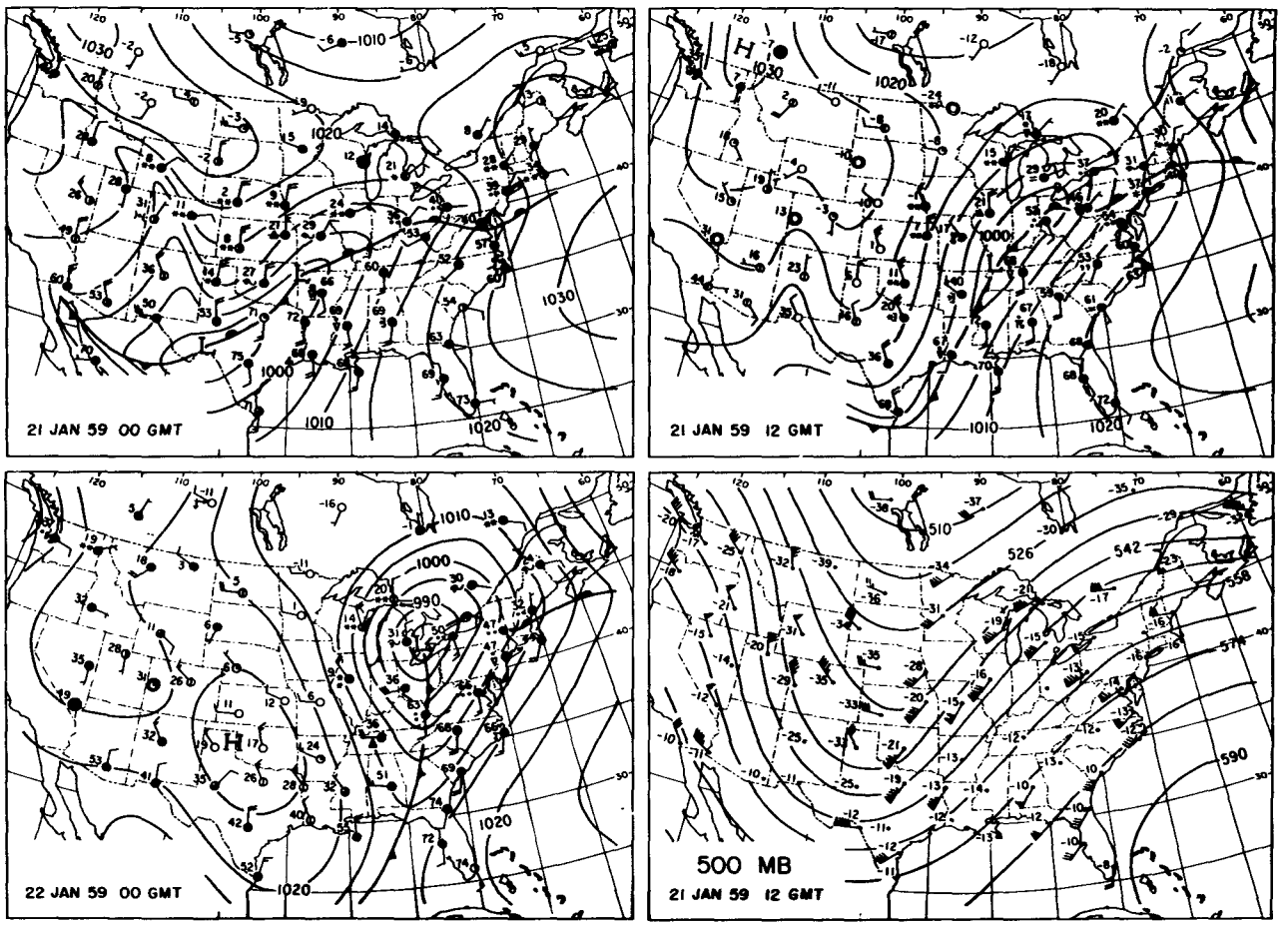

Fig. 4.1.1. Sequence of sea-level charts showing the development of a major cyclone. Lower right: 500 mb map at the onset of sudden cyclogenesis.

4. A CASE STUDY

4.1 General Synopsis

The case selected for study was a cyclone which developed rapidly over the central United States on January 21-22, 1959 (Fig. 4.1.1). The system was associated with an intense baroclinic zone and was accompanied by widespread heavy precipitation.

During the period 0000-1200 GMT of the 21st the frontal low moved from western Texas to southeastern Missouri, becoming more organized but filling slightly. Shortly after 1200 GMT the system began to deepen at the rate of approximately 1 mb hr^{-1}. By 0000 GMT of the 22nd it had reached southern Ontario and had then developed into a major cyclone. From the 500 mb map in the lower right of Fig. 4.1.1, it will be seen that, in accordance with Petterssen's development hypothesis (Petterssen, 1955), sudden development began when the area of appreciable vorticity advection in mid-troposphere spread over the low-level frontal zone.

An investigation of the dynamic and thermodynamic processes occurring in the atmosphere at the onset of sudden cyclogeneis should provide a better understanding of the complex phenomenon of cyclone development. It was therefore decided to perform the computations proposed in Section 3 using the data for 1200 GMT of the 21st.

Precipitation rates at 1200 GMT (Fig. 4.1.2) were obtained from the observed four-hour amounts ending at 1400 GMT which were then averaged over areas centered at grid points (see Fig. 4.3.1) and converted to hourly rates. The time and area averaging procedure resulted in the smooth pattern shown in Fig. 4.1.2. Note the elongation of the precipitation pattern along the

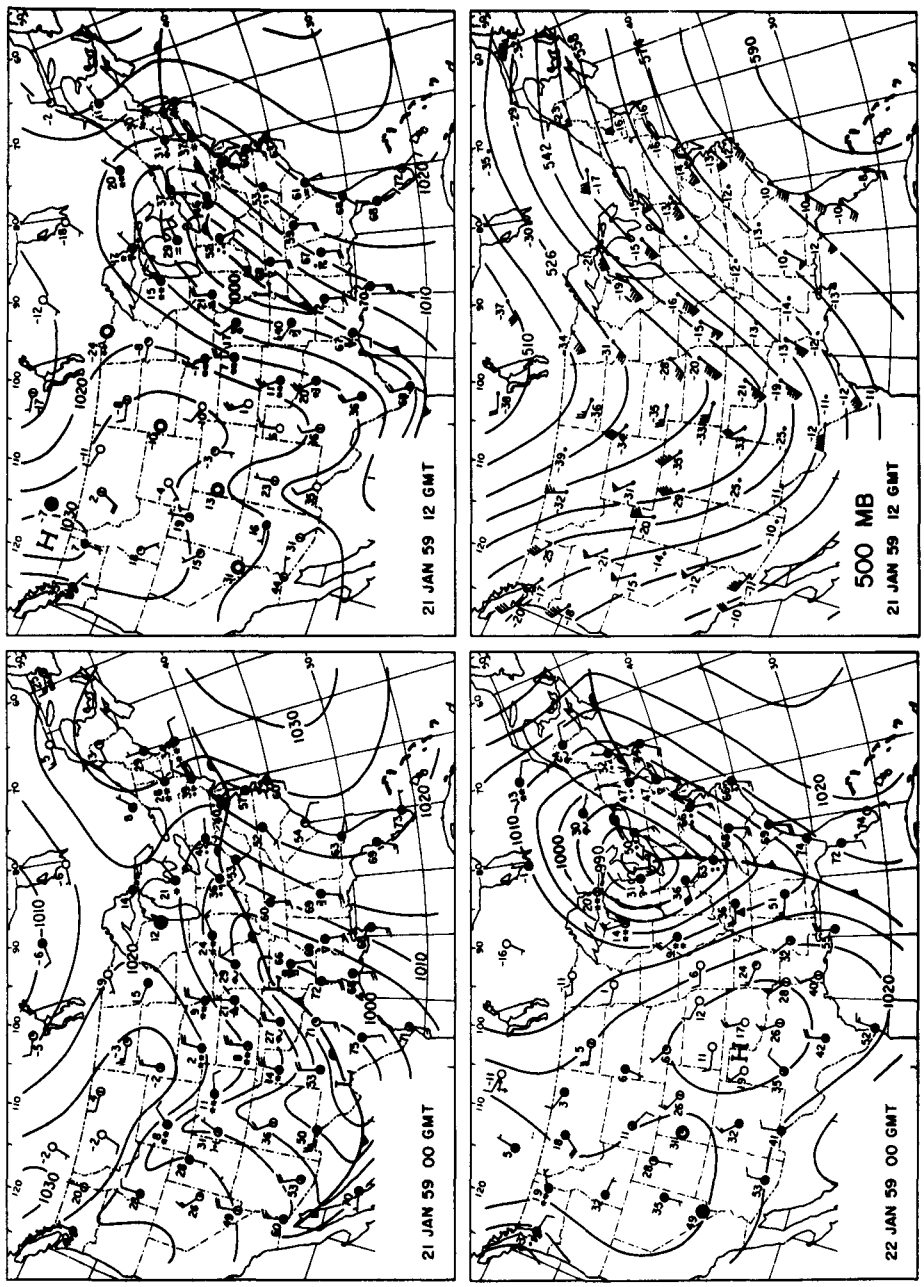

Fig. 4.1.1. Sequence of sea-level charts showing the development of a major cyclone. Lower right: 500 mb map at the onset of sudden cyclogenesis.

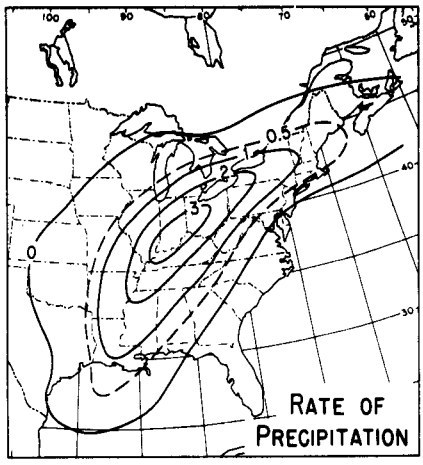

Fig. 4.1.2. Observed rate of precipitation. 1200 GMT Jan. 21, 1959. Units: mm hr^{-1}.

frontal zone. Furthermore, an examination of the surface data in Fig. 4.1.1 shows that most of the precipitation was in the form of rain, despite the fact that this was a mid-winter situation. A possible explanation of this is offered in Section 4.4.

4.2 Kinematically Computed Vertical Velocity

The vertical velocity was first computed kinematically at 900, 800, 600, 400, 300 and 200 mb by determining the divergence of the mean wind between successive levels. For the divergence calculations a nomogram similar to the one suggested by Fujita (1955) was used.

Orographic effects were included in the following manner. Let $p_s(x, y)$ be the surface pressure and let p_1 be a pressure level at which ω is to be determined. If $\partial p_s / \partial t = 0$,

$$\omega(p_1) = \nabla \cdot \hat{V}$$

where

$$\hat{V} = \int_{p_1}^{p_s} V \, \delta p$$

The above method has been used by a number of investigators (e. g., Rex, 1958, and Palmén and Holopainen, 1962).

In our computations p_s was put equal to the standard atmosphere pressure of the area-smoothed terrain provided by McClain (1960). The pressure at this smoothed topography varies from about 1000 to 700 mb over the United States, with a large area where $p_s > 900$ mb. If one used a constant p_1 over the entire region, the lowest convenient standard pressure level to be selected for p_1 would be 600 mb. However, if this value of p_1 were chosen, the vertical velocity at lower levels could not be obtained. It was therefore decided to vary p_1 over the region according to the following criteria:

$p_s > 900$ mb	$p_1 = 900$ mb
$900 > p_s > 800$ mb	$p_1 = 800$ mb
$p_s < 800$ mb	$p_1 = 600$ mb

The vertical velocity at higher levels was then computed in the customary manner by adding the divergence of the mean wind of successive layers.

The fields of vertical motion at 800, 600, 400 and 200 mb were then averaged over areas centered at grid points (see Fig. 4.3.1). The results for the region to the east of the Continental Divide are shown in Fig. 4.2.1.

The accuracy of any kinematic computation of the vertical velocity normally decreases with height. Furthermore, because of the sparsity of wind data in the region of maximum upward motion (see Fig. 4.1.1), our confidence in the kinematically computed values at 400 mb and especially at 200 mb is rather low. Nevertheless, the horizontal projections of the centers of maximum upward motion at 800, 600 and 400 mb agree fairly well with the center of heaviest precipitation (see Fig. 4.1.2). However, it became evident when computing the rate of release

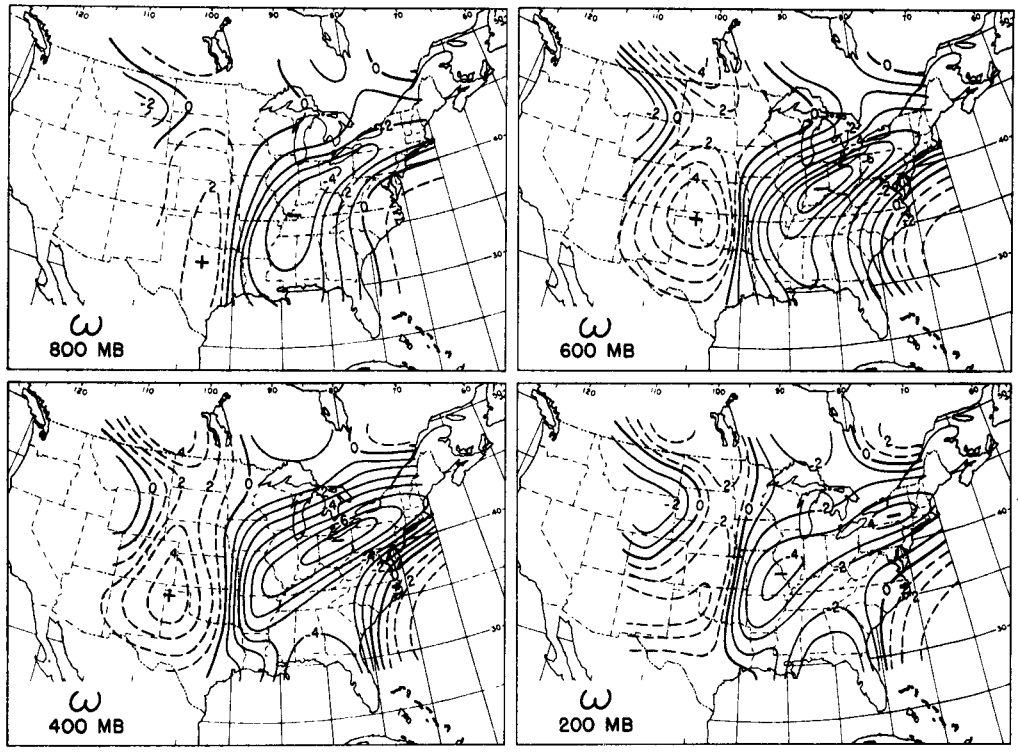

Fig. 4.2.1. Kinematically computed vertical velocity. 1200 GMT Jan 21, 1959. Units: 10^{-3} mb sec^{-1}.

of latent heat (described in Section 3.1) that in the region of maximum precipitation the kinematically computed vertical velocity accounted for only about 70 per cent of the observed precipitation. A possible reason for this discrepancy is that the strong low-level convergence in this area would indicate an appreciable import of liquid water in the form of stratus and stratocumulus clouds. According to Cunningham (1952) these clouds can contribute significantly to the precipitation.

It is of interest to note that precipitation occurred in Kansas and Oklahoma even though Fig. 4.2.1 shows downward motions at all levels in this region. This apparent inconsistency is likely caused by small-scale turbulence or orographic effects which are undetectable in the winds or smoothed topography used in the computations.

4.3 Vertical Velocity Due to Dry-Adiabatic Processes

Equation (3.1.4) was solved for the region shown in Fig. 4.3.1 using a vertical mesh size of 200 mb and keeping $\omega_a = 0$ at $p = 0$ and $p = 1000$ mb. The lateral boundaries, on which ω_a was set equal to zero, were located three grid distances outside the boundary of the region shown in Fig. 4.3.1.

In the terms on the right side of Eq. (3.1.4), the height data from nine levels (every 100 mb from 100 to 900 mb) were used. Let subscripts 1, 2, ..., 9 denote the levels $p = 100, 200, \ldots, 900$ mb. Then, in finite difference form,

$$\left(\frac{\partial^2 \omega_a}{\partial p^2}\right)_n \cong \frac{(\omega_a)_{n+2} + (\omega_a)_{n-2} - 2(\omega_a)_n}{(\Delta p)^2}$$

$$\left(V_g \cdot \nabla \frac{\partial z}{\partial p}\right)_n \cong (V_g)_n \cdot \nabla \frac{(z)_{n+1} - (z)_{n-1}}{\Delta p}$$

$$\left[\frac{\partial}{\partial p} V_g \cdot \nabla (q_g + f)\right]_n \cong \frac{\left[V_g \cdot \nabla (q_g + f)\right]_{n+1} - \left[V_g \cdot \nabla (q_g + f)\right]_{n-1}}{\Delta p}$$

where $\Delta p = 200$ mb, and n takes on the values 2, 4, 6 and 8. The customary finite difference approximations were used for the horizontal derivatives.

The values of σ were computed directly from the temperatures also using the data at nine levels from 100 to 900 mb. In finite difference form,

$$(\sigma)_n \cong - \frac{(\alpha)_n}{(\theta)_n} \frac{(\theta)_{n+1} - (\theta)_{n-1}}{\Delta p}$$

Equation (3.1.4) was first solved in the form

$$(4.3.1) \quad \sigma_o \nabla^2 \omega_a + f f_o \frac{\partial^2 \omega_a}{\partial p^2} = - g \nabla^2 V_g \cdot \nabla \frac{\partial z}{\partial p} + f \frac{\partial}{\partial p} V_g \cdot \nabla (q_g + f)$$

where $\sigma_o(p)$ is the area-averaged value of $\sigma(x, y, p)$. The solution at 600 mb is reproduced in Fig. 4.3.2. Comparing Figs. 4.3.2 and 4.2.1, it is evident that the solution of Eq. (4.3.1) grossly underestimates the magnitudes of the maximum downward and upward motion, especially that of the latter.

One reason for this discrepancy is due to the neglect of horizontal variations of σ. Fig. 4.3.3 shows the variations of σ / σ_o at 600 mb. This quantity varies from less than 0.5 to greater than 2.0. It will

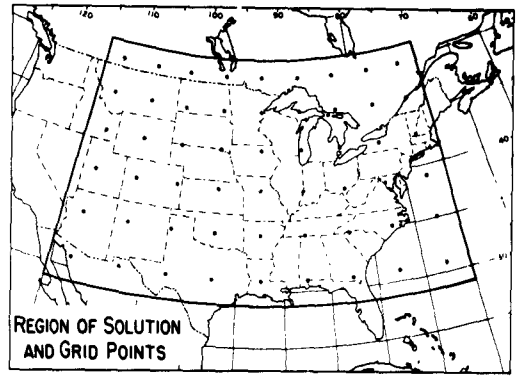

Fig. 4.3.1. Region of solution and grid points used for the numerical computations.

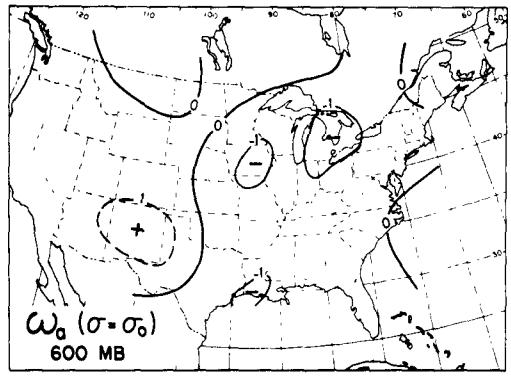

Fig. 4.3.2. Vertical velocity at 600 mb associated with dry-adiabatic processes keeping the static stability constant. 1200 GMT Jan. 21, 1959. Units: 10^{-3} mb sec^{-1}.

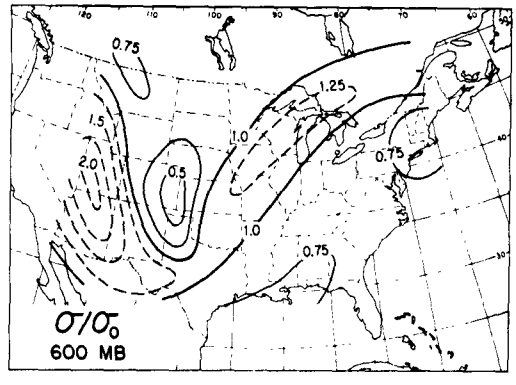

Fig. 4.3.3. Static stability at 600 mb divided by its areal average value. 1200 GMT Jan. 21, 1959.

be noted also that, as one might expect, the air in the frontal zone is more statically stable than either the warm or cold air.

Equation (3.1.4) was then solved, permitting σ to vary along the isobaric surfaces (Fig. 4.3.4). Comparing Figs. 4.3.4 and 4.3.2, it will be seen that one effect of letting σ vary is to shift the maxima of upward and downward motions towards regions of lower stability and to increase their magnitudes. This amplification is due to the circumstance that $\sigma/\sigma_0 < 1$ in these regions. Comparing Figs. 4.3.4 and 4.2.1, note that the magnitude of the maximum downward motion is correctly computed from Eq. (3.1.4) although the center is too far west. It is likely that inclusion of terrain effects in the numerical solution would have resulted in better agreement. The effect of neglecting orographic influences is especially noticable in the northwestern section of the region. However, the computed maximum of upward motion, though larger than in the case of constant static stability, is still seriously underestimated.

4.4 Effect of Release of Latent Heat on the Vertical Velocity

To solve Eq. (3.1.5), the rate of release of latent heat (H) must be known. This quantity was computed using the method described in Section 3.1; the results are shown in Fig. 4.4.1.

Equation (3.1.5) was then solved, permitting σ to vary and using the same region and boundary conditions as described in Section 4.3. The solution at 600 mb is presented in Fig. 4.4.2. The solutions at 800 and 400 mb were similar with maxima of about -3.5 and -4.0 x 10^{-3} mb sec^{-1}, respectively. Even though there was no release of latent heat at 200 mb, ω_h at this level was not zero. However, its magnitude was everywhere less than 0.3 x 10^{-3} mb sec^{-1}.

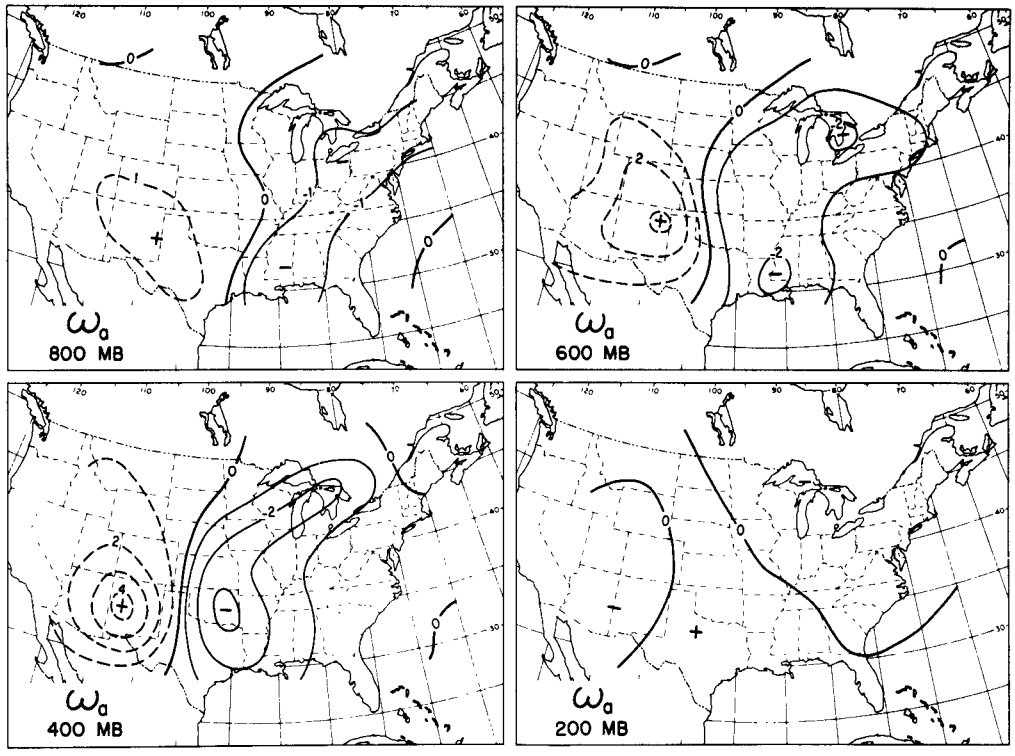

Fig. 4.3.4. Vertical velocity associated with dry-adiabatic processes permitting the static stability to vary. 1200 GMT Jan. 21, 1959. Units: 10^{-3} mb sec^{-1}.

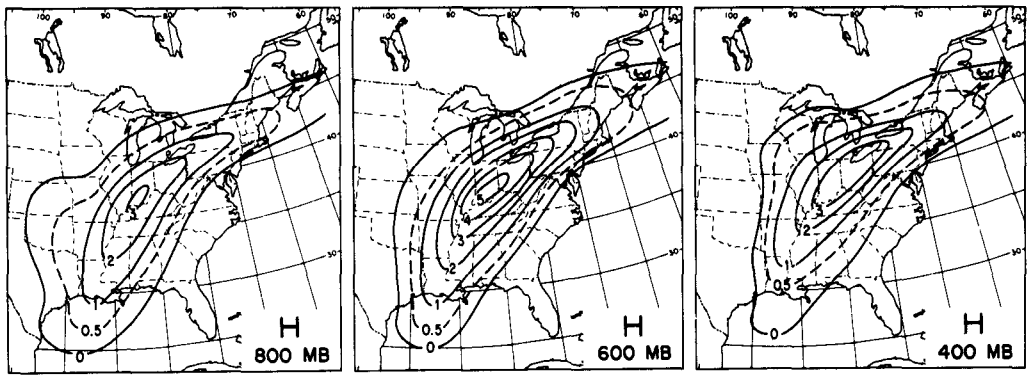

Fig. 4.4.1. Rate of release of latent heat computed from the observed precipitation. 1200 GMT Jan 21, 1959. Units: 10^3 ergs gm^{-1} sec^{-1}.

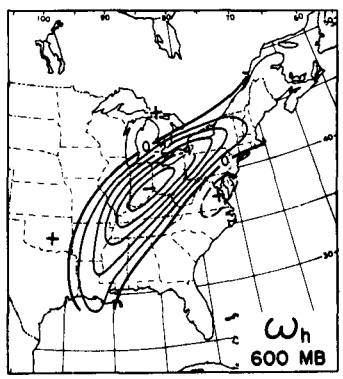

Fig. 4.4.2. Vertical velocity at 600 mb associated with saturated-adiabatic processes permitting the static stability to vary. 1200 GMT Jan. 21, 1959. Units: 10^{-3} mb sec^{-1}.

From Fig. 4.4.2 it will be seen that the effect of released latent heat is to amplify the upward motion in the region of heaviest precipitation and contribute to a slight downward motion in the surrounding region. This same effect has been observed by Smagorinsky (1956), Aubert (1957) and Pedersen (1962). Furthermore, this result is in agreement with the theoretical solution Eliassen (1959) obtained in considering the effect of an elliptically-shaped heat source in a baroclinic zonal current.

A possible explanation why the precipitation in the case studied was predominantly rain is the following. If there exists initially a large region of relatively uniform upward motion such as that given by Fig. 4.3.4 in the region of heaviest precipitation, the vertical velocity will be amplified in those areas which first attain saturation and damped in the surrounding areas. In the case under study, condensation presumably first occurred in the maritime tropical air near the front, producing rain. Further north, where the temperatures were low enough to yield snow, the upward motion was decreased and the attainment of saturation delayed.

The solutions of Eqs. (3.1.4) and (3.1.5), permitting σ to vary in both equations, were added; the results are shown in Fig. 4.4.3. Comparing Figs. 4.4.3 and 4.2.1 we see that the agreement is satisfactory at 800 and 600 mb, except that the numerical solutions still give the maximum downward motion too far west and do not detect the orographically induced upward motion in the northwest section of the region. The maximum upward motion is slightly underestimated but this would be expected since frictional convergence has been neglected. The agreement is poorer at 400 and more so at 200 mb. However, as has been pointed out in Section 4.2, our confidence in the kinematically computed vertical velocities at these levels is rather low.

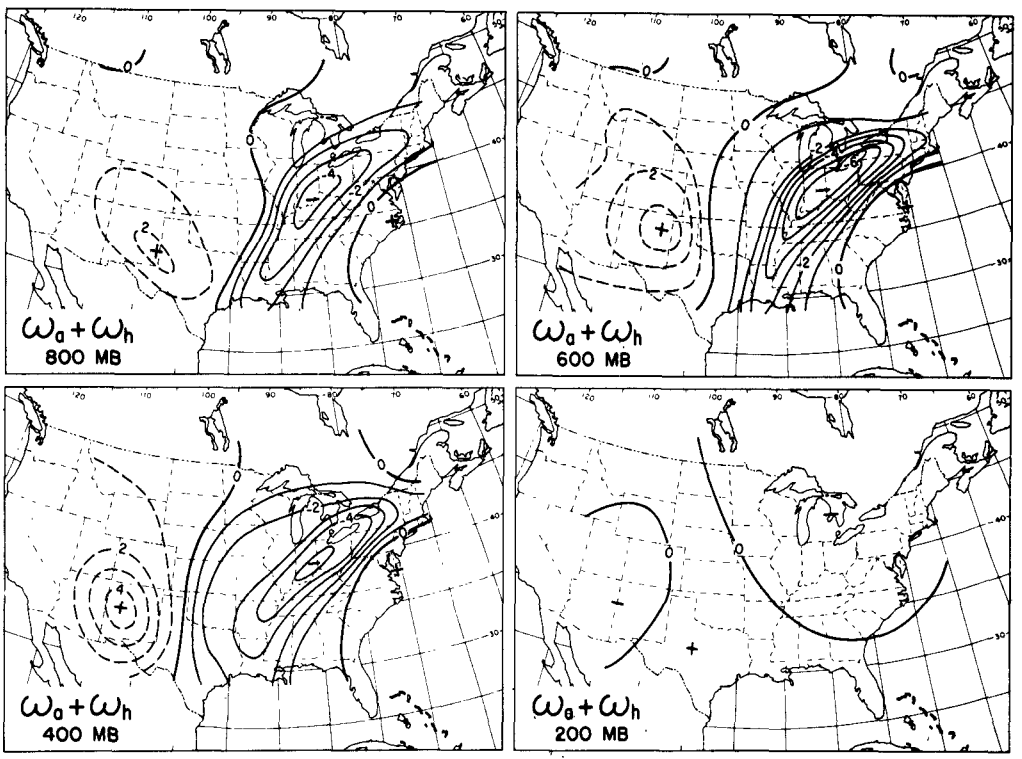

Fig. 4.4.3. Sum of the vertical velocities associated with dry- and saturated-adiabatic processes permitting the static stability to vary. 1200 GMT Jan. 21, 1959. Units: 10^{-3} mb sec^{-1}.

To sum up, it can be stated that, in regions of heavy precipitation, one cannot compute the vertical velocity with adequate accuracy by numerical means unless one includes the effect of released heat of vaporization.

4.5 Influence of Released Latent Heat on the Changes in Kinetic Energy

The induced ageostrophic wind components V_a' and V_h' were determined from Eqs. (3.2.4) and (3.2.5) at 900, 700, 500 and 300 mb using the values of ω_a and ω_h obtained from the solutions of Eqs. (3.1.4) and (3.1.5). The results at 900 and 300 mb are shown in Fig. 4.5.1. Note the reversal in direction of both V_a' and V_h' between the two levels.

The right hand sides of Eqs. (3.2.9) to (3.2.11) were then evaluated over the region given in Fig. 4.3.1 for four layers, each 200 mb deep, between 1000 and 200 mb. Table 4.5.1 shows the results of computing these quantities and adding them to obtain

$$\frac{\partial K_g}{\partial t} = \left[\frac{\partial K_g}{\partial t}\right]_g + \left[\frac{\partial K_g}{\partial t}\right]_a + \left[\frac{\partial K_g}{\partial t}\right]_h \tag{4.5.1}$$

The table also shows the amount of kinetic energy, the time required for the kinetic energy to double (assuming $\partial K_g / \partial t$ to be constant), and the total rate of release of latent heat within each layer (H_t). For convenience, the layers are identified by numbers, thus: 1 (1000 to 800 mb); 2 (800 to 600 mb); 3 (600 to 400 mb); and 4 (400 to 200 mb).

Table 4.5.1. Comparison of the terms in Eq. (4.5.1). For definition of symbols, see text.

Term	Units	Layer				Totals
		1	2	3	4	
K_ζ	10^{25} ergs	1.95	3.50	9.57	18.44	33.46
H_t	10^{20} ergs sec^{-1}	27.9	77.1	86.5	37.2	228.7
$[\partial K_\zeta/\partial t]_\zeta$	10^{20} ergs sec^{-1}	0.34	0.57	1.23	-0.01	2.13
$[\partial K_\zeta/\partial t]_a$	10^{20} ergs sec^{-1}	1.26	1.09	3.01	3.89	9.25
$[\partial K_\zeta/\partial t]_h$	10^{20} ergs sec^{-1}	1.28	-0.39	0.54	3.05	4.48
$\partial K_\zeta/\partial t$	10^{20} ergs sec^{-1}	2.88	1.27	4.78	6.93	15.86
Doubling time	hours	18.8	76.4	55.7	73.7	58.4

The effect of neglecting surface friction is reflected in the small doubling times computed for layer 1. However, the doubling times computed for layers 2, 3 and 4 appear reasonable, although there is some variation which can be attributed to one or more of the following causes:

(i) horizontal import of kinetic energy by the ageostrophic wind;

(ii) rate of working by the pressure due to the rotational component of the ageostrophic wind; and

(iii) errors arising from inaccuracy in the input data.

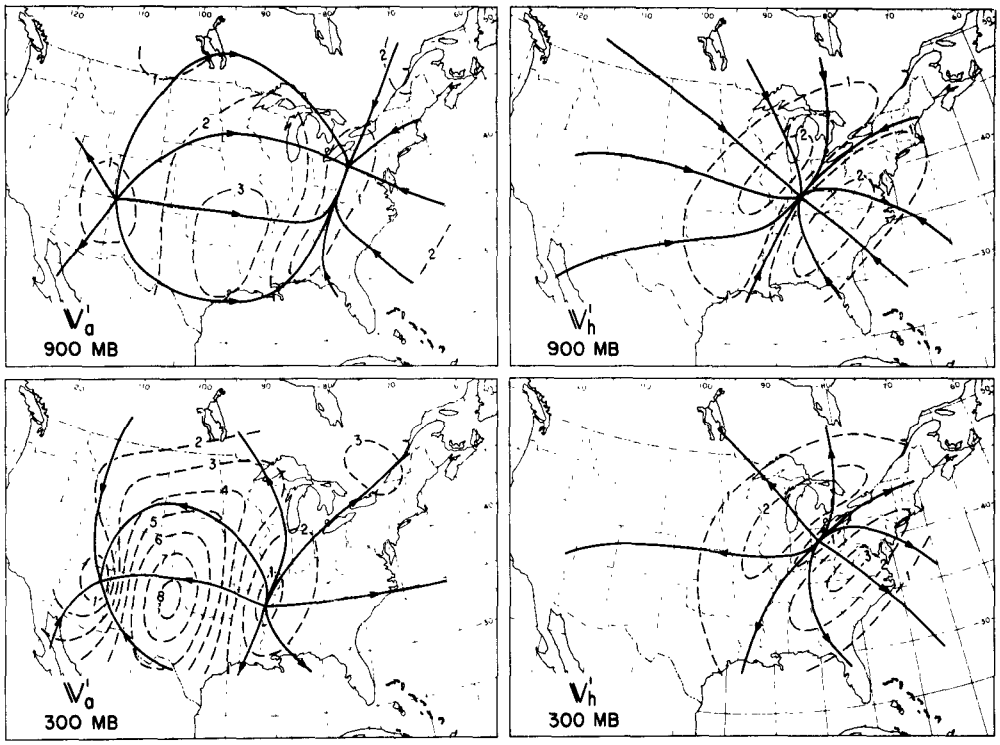

Fig. 4.5.1. Irrotational ageostrophic wind components at 900 and 300 mb. The charts on the left and right show the components associated with dry- and saturated-adiabatic processes, respectively. Solid lines: streamlines. Dashed lines: isotachs in units of m sec^{-1}. 1200 GMT Jan. 21, 1959.

It may be noted also that in each layer H_t is an order of magnitude larger than $\partial K_\zeta / \partial t$. Comparing $[\partial K_\zeta / \partial t]_a$ and $[\partial K_\zeta / \partial t]_h$ we see that in layers 1 and 4, both terms are approximately equal, although at mid-levels $[\partial K_\zeta / \partial t]_h$ is rather small and is actually negative in layer . .

Further insight is gained if the individual terms in Eqs. (3.2.10) and (3.2.11) are examined. Let us write these equations symbolically as

(4.5.2) $$\left[\frac{\partial K_\zeta}{\partial t}\right]_a = I_{va} + W_a$$

(4.5.3) $$\left[\frac{\partial K_\zeta}{\partial t}\right]_h = I_{vh} + W_h$$

where I_{va} and I_{vh} represent the net vertical import of kinetic energy by ω_a and ω_h respectively, and W_a and W_h denote the rate of working by the pressure by Ψ'_a and Ψ'_h . The results are shown in Table 4.5.2.

Table 4.5.2. Comparison of the terms in Eqs. (4.5.2) and (4.5.3). For definition of symbols, see text. Units: 10^{20} ergs sec^{-1}.

Term	Layer				Totals
	1	2	3	4	
I_{va}	-0.59	-0.66	-0.03	0.43	-0.86
W_a	1.85	1.75	3.04	3.47	10.11
I_{vh}	-0.47	-0.88	-0.18	0.87	-0.29
W_h	1.75	0.49	0.36	2.18	4.78

The terms I_{va} and I_{vh} are negative in the lower troposphere and positive at higher levels, indicating a net transport of kinetic energy from the lower to upper troposphere. Moreover, they are generally of smaller magnitude than the terms W_a and W_h. These latter terms are positive at all levels. The mid-troposphere minimum of $[\partial K_g / \partial t]_h$, noted above, evidently results from W_h. The vertical variation of this last term can be readily explained.

At mid-levels, where the rate of release of latent heat is a maximum, $\partial \omega_h / \partial p$ is near zero. Consequently the induced ageostrophic velocity V_h' is small, and therefore so is W_h.

At low levels, the center of maximum convergence caused by released latent heat is located in a region of relatively low contour heights. The induced inflow (see Fig. 4.5.1) towards this center is therefore generally in the direction of decreasing pressure, resulting in positive work being done on the air parcels.

At high levels, the center of maximum divergence is situated in a region of relatively high contour heights. This is because in the upper troposphere a warm ridge lies just east of the location of the surface frontal low. Hence the induced outflow is again generally in the direction of decreasing pressure.

The term W_a has a similar, though less pronounced, vertical variation.

Although only one case has been investigated here, it is likely that similar results would be obtained from further studies. It is typical of frontal systems that precipitation occurs in a region of relatively low contour heights in the lower troposphere surmounted by a warm ridge at higher levels. Therefore it is to be expected that in such systems accompanied by moderate or heavy precipitation, released latent heat makes a significant contribution to the kinetic energy changes at low and high levels but has little effect in mid-troposphere.

Next, the energy conversion integrals

$$C_a = -\int\int \omega_a \alpha \, \delta A \, \frac{\delta p}{g} \tag{4.5.4}$$

and

$$C_h = -\int\int \omega_h \alpha \, \delta A \, \frac{\delta p}{g} \tag{4.5.5}$$

were computed. The results are shown in Table 4.5.3.

Table 4.5.3. Comparison of Eqs. (4.5.4) and (4.5.5). Units: 10^{20} ergs sec^{-1}.

Term	Layer				Totals
	1	2	3	4	
C_a	0.46	8.28	25.92	37.63	72.29
C_h	8.76	27.71	40.77	33.15	110.39

Except at level 4, the contribution of released latent heat to the energy conversion processes exceeds that caused by dry-adiabatic motion. Comparing the values in Table 4.5.3 with the computed magnitudes of $[\partial K_g/\partial t]_a$ and $[\partial K_g/\partial t]_h$ given in Table 4.5.1, it is evident that the other terms in Eqs. (3.2.13) and (3.2.14) (not computed) must in general be of opposite sign to C_a and C_h.

4.6 The Role of Released Latent Heat in Vorticity Production

The change in absolute vorticity following the motion of the sea-level center (see Fig. 4.1.1) between 0000 GMT of the 21st and 0000 GMT of the 22nd was observed to be

$$\frac{\delta}{\delta t}(q_g + f) = 0.88 \times 10^{-4} \text{ sec}^{-1} \text{ (24 hr)}^{-1} \tag{4.6.1}$$

Since the rate of change of vorticity was fairly uniform throughout the 24-hour period, the value given by Eq. (4.6.1) may be taken as the instantaneous rate of change at 1200 GMT of the 21st.

The right hand sides of Eqs. (3.3.5) and (3.3.6) were computed from conditions at 1200 GMT of the 21st, using the following numerical values:

$q_g = 1.79 \times 10^{-4}$ sec^{-1} $\qquad$ $V = 20$ m sec^{-1}

$f = 0.87 \times 10^{-4}$ sec^{-1} $\qquad$ $\partial\omega_a/\partial p = 0.4 \times 10^{-5}$ sec^{-1}

$C = 0.005$ $\qquad$ $\partial\omega_h/\partial p = 1.5 \times 10^{-5}$ sec^{-1}

$V_o = 10$ m sec^{-1}

The numerically computed convergence

$$\frac{\partial\omega_a}{\partial p} + \frac{\partial\omega_h}{\partial p} = 1.9 \times 10^{-5} \text{ sec}^{-1}$$

agreed well with the value determined directly from the wind observations (2.3×10^{-5} sec^{-1}). The following results were obtained:

$$\mathbf{k} \cdot \nabla \times \mathbf{F} = -3.87 \times 10^{-4} \text{ sec}^{-1} \text{ (24 hr)}^{-1}$$

$$(q_g + f)(\partial\omega_a/\partial p) = 0.92 \times 10^{-4} \text{ sec}^{-1} \text{ (24 hr)}^{-1}$$
$$(q_g + f)(\partial\omega_h/\partial p) = 3.45 \times 10^{-4} \text{ sec}^{-1} \text{ (24 hr)}^{-1}$$

Thus

$$(4.6.2)\quad \left[\frac{\delta}{\delta t}(q_g+f)\right]_a + \left[\frac{\delta}{\delta t}(q_g+f)\right]_h = 0.50 \times 10^{-4} \text{ sec}^{-1} \text{ (24 hr)}^{-1}$$

In view of the approximations made in computing the term $\mathbf{k} \cdot \nabla \times \mathbf{F}$, the agreement between the values given by Eqs. (4.6.2) and (4.6.1) must be considered fortuitous. Nevertheless, the frictional term must be large to compensate for the tendency for rapid intensification resulting from convergence. Thus the observed changes in vorticity evidently resulted from a small imbalance between two large quantities, production of vorticity by convergence and destruction by friction.

If condensation suddenly ceased in the system,

$$\frac{\delta}{\delta t}(q_g + f) = \left[\frac{\delta}{\delta t}(q_g + f)\right]_a$$
$$= -2.95 \times 10^{-4} \text{ sec}^{-1} \text{ (24 hr)}^{-1}$$

which would correspond to rapid weakening. Conceivably this could be one reason, along with an increased drag coefficient, for the rapid decay observed when hurricanes enter land and are cut off from their moisture supply. It is not intended to imply that the quasi-geostrophic equations (3.1.4) and (3.1.5) are necessarily adequate in the case of a hurricane to depict the fields

of vertical motion and convergence. Nevertheless, in a hurricane one would expect released latent heat to have an effect on these fields similar to that demonstrated in this paper.

Since even small values of low-level convergence (of the order of 0.5 to 1.0×10^{-5} sec^{-1}) would by themselves produce vorticity changes larger than those observed in the atmosphere, it is likely that at all stages in the evolution of a low the opposing effects of friction and convergence very nearly balance. The initiation of condensation would then result in an imbalance and an intensification of the system with an accompanying change in the frictional effect, caused by a modification of the velocity field, restoring the state of near-balance.

5. CONCLUDING REMARKS

Although only one synoptic situation has been examined here, the results appear general enough to permit the tentative conclusion that they are typical of lows associated with strong baroclinity and accompanied by moderate to heavy precipitation. The results for the case investigated may be summarized as follows.

In the case studied, the conventional method of obtaining the vertical velocity from the diagnositc ω -equation by assuming constant static stability and dry-adiabatic motion proved to be inadequate. The maximum upward motion obtained in this way was only about one-fourth of the value computed by the kinematic method. Only by permitting the static stability to vary and by including the influence of released latent heat (the latter modification being the more important) was satisfactory agreement between the numerically and kinematically computed values obtained.

Accompanying the amplifying effect that released heat of vaporization has on the vertical velocity in mid-troposphere was an increase in low-level convergence and high-level divergence. Furthermore, owing to the circumstance that the precipitation was associated with a region of relatively low contour heights in the lower troposphere surmounted by a warm ridge at higher levels, the induced ageostrophic horizontal motion was in the direction of decreasing pressure at both low and high levels, resulting in production of kinetic energy. This production was of the same order of magnitude as that caused by dry-adiabatic processes. At middle levels, released latent heat had little effect on the changes in kinetic energy.

The maximum low-level convergence associated with release of latent heat was about three times as large as that arising from dry-adiabatic processes, excluding frictional convergence. One might therefore conclude that the production of vorticity was closely related to the rate of release of latent heat. Since the vorticity production predicted by the numerically computed convergence, which agreed well with the value calculated directly from the observed winds, greatly exceeded the observed production, one might further conclude that this production was very nearly balanced by frictional effects.

It should be pointed out that the modifying effects of released heat of vaporization can come into play only after development has begun and condensation has been achieved. Therefore one cannot say that released latent heat initiates cyclones but rather that it affects their subsequent growth.

REFERENCES TO LITERATURE

Aubert, E. F., 1957: On the release of latent heat as a factor in large scale atmospheric motions. J. Meteor., 14, pp. 527-542.

Cunningham, R. M., 1952: The distribution and growth of hydrometeors around a deep cyclone. MIT Tech. Rep. No. 18, Contract No. DA-36-039-sc-124, May, 1952.

Eliassen, A., 1959: On the formation of fronts in the atmosphere. The Rossby Memorial Volume, The Rockefeller Institute Press and Oxford University Press, pp. 277-287.

Ferrel, W., 1889: A Popular Treatise on the Winds, John Wiley and Sons.

Fjörtoft, R., 1955: On the use of space-smoothing in physical weather forecasting. Tellus, 7, pp. 462-480.

Fujita, T., 1955: Results of detailed synoptic studies of squall lines. Tellus, 7, pp. 405-436.

Fulks, J. R., 1935: Rate of precipitation from adiabatically ascending air. Monthly Wea. Rev., 63, pp. 291-294 (see also Smithson. Met. Tables, 1951, pp. 325-326).

Hann, J. von, 1874: Über den Einfluss des Regens auf den Barometerstand und über die Entstehung der Niederschläge im Allgemeinen. Zeit. d. Österreich. Gesellschaft für Met., 9, pp. 289-294.

Hollmann, G., 1956: Über prinzipielle Mängel der geostrophischen Approximation und die Einführung ageostrophischer Windkomponenten. Meteor. Rundschau, 9, pp. 73-78.

Lorenz, E. N., 1960: Energy and numerical weather prediction. Tellus, 12, pp. 364-373.

Manabe, S., 1956: On the contribution of heat released by condensation to the change in pressure pattern. JMS of Japan, Ser. II, 34, pp. 308-320.

Margules, M., 1903: Über die Energie der Stürme. Jahr. kais-kön Zent. für Met., Vienna (English translation by C. Abbe in Smithson. Misc. Coll., 51, 1910, pp. 533-595).

_____, 1906: Zur Sturmtheorie. Met. Zeit., 13, pp. 481-497.

McClain, E. P., 1960: Some effects of the western cordillera of North America on cyclone activity. J. Meteor., 17, pp. 104-115.

Palmén, E., and E. O. Holopainen, 1962: Divergence, vertical velocity and conversion between potential and kinetic energy in an extra-tropical disturbance. Geophysica, 8, pp. 89-113.

Pedersen, K., 1962: An experiment in quantitative precipitation forecasting with a quasi-geostrophic model. Univ. of Chicago Sci. Rep. No. 1, NSF Grant G 17953, Oct., 1962.

Petterssen, S., 1953: On the relation between vorticity, deformation and divergence and the configuration of the pressure field. Tellus, 5, pp. 231-237.

_____, 1955: A general survey of factors influencing development at sea level. J. Meteor., 12, pp. 36-42 (see also Weather Analysis and Forecasting, I, McGraw Hill, 1956, pp. 320-339).

_____, D. L. Bradbury, and K. Pedersen, 1962: The Norwegian cyclone models in relation to heat and cold sources. Geof. Publ., 25 (The Bjerknes Memorial Volume), pp. 243-280.

Phillips, N. A., 1956: The general circulation of the atmosphere: a numerical experiment. Quart. Journ. Roy. Met. Soc., 82, pp. 123-164.

Refsdal, A., 1930: Der feuchtlabile Niederschlag. Geof. Publ. 5, No. 12.

Rex, D. F., 1958: Vertical atmospheric motion in the Equatorial Central Pacific. Geophysica, 6, pp. 479-500.

Reye, Th., 1865: Die Ausdehnung der atmosphärischen Luft bei der Wolkenbildung. Annalen der Physik, 125, pp. 618-626.

_____, 1872: Die Wirbelstürme, Tornados und Wettersäulen. Verlag Carl Rumpler, Hannover.

Smagorinsky, J., 1956: On the inclusion of moist adiabatic processes in numerical prediction models. Ber. d. deutsches Wetterd., 38, pp. 82-90.

Smebye, S., 1958: Computation of precipitation from large scale vertical motion. J. Meteor., 15, pp. 547-560.

White, R. M., and B. Saltzman, 1956: On the conversion between potential and kinetic energy in the atmosphere. Tellus, 8, pp. 357-363.

Wiin-Nielsen, A., 1959: On certain integral constraints for the time integration of baroclinic models. Tellus, 11, pp. 45-49.